ISSN: 2476-6909; Modares. Mech. Eng. *2026;26(09):725-732.*

Modares Mechanical Engineering

DOI: 10.48311/mme.2026.96872.0

journal homepage: www.mme.modares.ac.ir

Automated Air curtain for Enhanced Air Condition in Enclosed Spaces Based on Sliding Mode Control

Amirreza Mirzajani, Ghazaleh Babazadeh Asbagh, Sevda Rezazadeh Movahhed, Mohammad Ali Hamed*, Moharram Jafari

Mechanical Engineering, University of Tabriz, Tabriz, Iran

ARTICLE INFO

Article Type
Original Research

Article History
Received: June 17, 2025
Revised: January 26, 2026
Accepted: February 11, 2026
ePublished: June 20, 2026

ABSTRACT

Air curtains are commonly employed in a variety of applications, including industrial ventilation systems, commercial buildings, fire safety measures, and smoke control systems. These devices are particularly effective in creating an invisible barrier of high-velocity air that separates indoor and outdoor environments. This barrier significantly reduces the infiltration of external air, thereby limiting the spread of pollutant gases within enclosed spaces. In addition to improving indoor air quality, air curtains contribute to temperature regulation and energy efficiency by minimizing air leakage and reducing heat transfer across the separation boundary. This study focuses on enhancing the performance of air curtains for pollutant containment, specifically the control of CO_2 gas mass fraction under varying air and pressure conditions that act as external disturbances. To achieve this, a sliding mode control (SMC) method is integrated into the regulation mechanism of the air curtain velocity. The SMC approach is known for its robustness and effectiveness in handling systems with high degrees of uncertainty or external perturbations. A wall jet configuration of the air curtain, combined with the SMC strategy, is subjected to comprehensive numerical simulations. These simulations evaluate the system's ability to maintain effective pollutant separation and control in dynamically changing environments. The results demonstrate that the proposed control system significantly enhances the stability and performance of the air curtain, ensuring consistent pollutant containment. Even under critical pressure fluctuations, the system maintains optimal functionality, offering improved safety, and operational efficiency.

Keywords: air curtain, air condition monitoring, pollutant gas containment, turbulence, sliding mode control

How to cite this article
Mirzajani A.R, Babazadeh Asbagh Gh, Rezazadeh Movahhed S, Hamed M.A, Jafari M, Automated Air curtain for Enhanced Air Condition in Enclosed Spaces Based on Sliding Mode Control. Modares Mechanical Engineering; *2026;26(09):725-732.*

**Corresponding author's email: ma.hamed@tabrizu.ac.ir*
**Corresponding ORCID ID: 0000-0003-0942-8604*

شاپا: ۷۹۰۹-۲۴۷۶؛ مهندسی مکانیک مدرس. ۷۳۲-۷۲۵:(۰۹)۲۶؛۱۴۰۵

مهندسی مکانیک مدرس

DOI: 10.48311/mme.2026.96872.0

صفحه اصلی مجله: mme.modares.ac.ir

پرده هوای خودکار برای بهبود شرایط تهویه در فضاهای بسته بر پایه کنترل مود لغزشی

امیررضا میرزاجان، غزاله بابازاده اسبق، سئودا رضازاده موحد، محمدعلی حامد*، محرم جعفری

گروه مهندسی مکانیک، دانشگاه تبریز، تبریز، ایران

اطلاعات مقاله

نوع مقاله

مقاله پژوهشی

تاریخچه مقاله

دریافت: ۱۴۰۴/۰۳/۲۷

بازنگری: ۱۴۰۴/۱۱/۰۶

پذیرش: ۱۴۰۴/۱۱/۲۲

ارائه آنلاین: ۱۴۰۵/۰۳/۳۰

چکیده

پرده‌های هوا معمولا در کاربردهای مختلفی از جمله سیستم‌های تهویه صنعتی، ساختمان‌های تجاری، اقدامات ایمنی در برابر آتش و سامانه‌های کنترل دود مورد استفاده قرار می‌گیرند. این تجهیزات به‌ویژه در ایجاد یک مانع نامرئی از جریان هوای پرسرعت که محیط‌های داخلی و خارجی را از یکدیگر جدا می‌کند، بسیار مؤثر هستند. این مانع به‌طور قابل‌توجهی نفوذ هوای بیرونی را کاهش داده و در نتیجه از انتشار گازهای آلاینده در فضاهای بسته جلوگیری می‌کند. علاوه بر بهبود کیفیت هوای داخل، پرده‌های هوا با کاهش نشت هوا و انتقال حرارت در مرز جدایش، به تنظیم دما و افزایش بهره‌وری انرژی نیز کمک می‌کنند.

این مطالعه بر بهبود عملکرد پرده‌های هوا در مهار آلاینده‌ها، به‌ویژه کنترل کسر جرمی گاز دی‌اکسید کربن تحت شرایط متغیر جریان هوا و فشار که به‌عنوان اغتشاشات خارجی عمل می‌کنند، تمرکز دارد. برای دستیابی به این هدف، روش کنترل مود لغزشی در مکانیزم تنظیم سرعت پرده هوا به کار گرفته شده است. این روش به مقاوم بودن و کارایی بالا در مواجهه با سیستم‌های دارای عدم قطعیت بالا یا اغتشاشات خارجی شناخته می‌شود.

در این پژوهش، ساختار جت دیواره‌ای پرده هوا همراه با رویکرد کنترل مود لغزشی از طریق شبیه‌سازی‌های عددی جامع مورد بررسی قرار گرفته است. این شبیه‌سازی‌ها توانایی سیستم در حفظ جداسازی مؤثر آلاینده‌ها و کنترل آن‌ها را در شرایط محیطی پویا ارزیابی می‌کنند. نتایج نشان می‌دهد که سیستم کنترلی پیشنهادی به‌طور قابل‌توجهی پایداری و عملکرد پرده هوا را بهبود می‌بخشد و مهار مداوم آلاینده‌ها را تضمین می‌کند. حتی در شرایط نوسانات شدید فشار، سیستم عملکرد بهینه خود را حفظ کرده و ایمنی و کارایی عملیاتی را افزایش می‌دهد.

کلیدواژه‌ها: پرده هوا، پایش تهویه، مهار گازهای آلاینده، آشفتگی، کنترل مود لغزشی

نحوه ارجاع به این مقاله

میرزاجان امیررضا، بابازاده اسبق غزاله، رضازاده موحد سئودا، حامد محمدعلی، جعفری محرم، پرده هوای خودکار برای بهبود شرایط تهویه در فضاهای بسته بر پایه کنترل مود لغزشی ، مهندسی مکانیک مدرس. ۷۳۲-۷۲۵:(۰۹)۲۶؛۱۴۰۵

*پست الکترونیکی نویسنده عهده‌دار مکاتبات: ma.hamed@tabrizu.ac.ir

*شناسه ارکید نویسنده عهده‌دار مکاتبات: 0000-0003-0942-8604

1- Introduction

Enhancing air condition management within enclosed or semi-enclosed spaces has become a critical objective across a wide range of sectors, including industrial facilities, commercial buildings, and public safety infrastructure. The ability to effectively manage airborne pollutants, such as hazardous gases, particulate matter, and smoke is essential for maintaining not only occupant health and safety but also for achieving regulatory compliance and operational efficiency. In this context, air curtains have emerged as a practical and widely adopted solution. These devices generate a high-velocity, laminar sheet of air that acts as an invisible barrier at doorways or openings, effectively separating indoor environments from external conditions [1]. By doing so, air curtains significantly reduce the infiltration of unwanted substances such as dust, fumes, and outdoor pollutants.

Beyond their role in pollutant exclusion, air curtains offer multiple operational benefits, including temperature regulation, reduction of conditioned air loss, and enhancement of overall energy efficiency within controlled environments. They are extensively utilized in applications ranging from industrial ventilation systems and commercial entrances to fire safety and smoke control systems, where maintaining zone integrity is essential. Nevertheless, one of the major challenges in air curtain design and implementation is ensuring consistent and optimal performance under varying and often unpredictable environmental conditions, such as fluctuating pressure gradients, temperature differentials, and external wind loads. To address these challenges, some investigations are conducted on the optimization of air curtain configurations and control strategies.

Ji et al. [2] developed a novel air curtain system, known as a push-pull air curtain, and evaluated its effectiveness in smoke control within a tunnel. Their findings indicated that push-pull air curtains outperformed conventional side-wall smoke exhaust methods. Additionally, the study examined the impact of air outlet velocity and the momentum ratio between the outgoing airflow and incoming smoke.

Safarzadeh et al. [3] investigated the role of vertical and horizontal air curtains in fire control for multi-storey buildings. Their research revealed that vertical air curtains performed poorly under low-ventilation conditions. Expanding on this work, Safarzadeh et al. [4] further explored the influence of air curtains on fire spread in multi-floor structures, analyzing the effects of supply angles, velocity, and ventilation on pollutant distribution and temperature regulation. Their results showed that under adequate ventilation conditions, the mass fraction of pollutant gases (CO and CO_2) approached zero, whereas in poorly ventilated environments, air curtain efficiency significantly decreased.

Yu et al. [5] examined the performance of PID-controlled air curtains in urban bifurcated tunnels, highlighting a strong correlation between fire source position, heat release rate, and air curtain flow rate. Zhang et al. [6] assessed the effect of air curtain jet velocity on smoke control in tunnels, concluding that a minimum jet velocity of 14 (m/s) was required for effective containment. Viegas [7] investigated the application of downward vertical air curtains as a method for preventing smoke movement within buildings, demonstrating their efficiency in smoke containment. Additionally, Zhang et al. [8] analyzed the use of air curtain-based smoke control systems in subway platforms, confirming their effectiveness in preventing smoke diffusion.

Most of the previous researches on air curtains have predominantly concentrated on optimizing their physical and geometric configurations to improve performance across different applications. Key areas of focus have included outlet velocity profiles, jet inclination angles, nozzle geometries, and the development of novel structural designs, such as the push-pull air curtain systems which aim to enhance the stability and penetration of the air jet.

Despite these advancements, there remains a noticeable gap in the integration of advanced control methodologies aimed at adapting air curtain performance in real-time to fluctuating environmental conditions. Most conventional approaches treat the air curtain as a passive device with fixed operational parameters, which limits its effectiveness in the presence of external disturbances such as sudden pressure shifts, varying pollutant loads, or temperature gradients.

This highlights the need for advanced control strategies that can dynamically adjust air curtain parameters in response to real-time environmental feedback. Such methods could significantly enhance the functionality and reliability of air curtains, especially in critical scenarios requiring precise pollutant containment or thermal separation.

In air curtain jet systems, pressure variations act as disturbances that can introduce nonlinear effects on curtain velocity, making it difficult to predict and control using traditional methods like PID. Since PID controllers are designed for linear systems, they often struggle to maintain stability when faced with variable pressure conditions. In contrast, SMC is a more effective solution due to its robust handling of nonlinear disturbances and variations [9]. SMC allows for precise and stable regulation of air curtain velocity, even under continuous pressure variation. Additionally, SMC is computationally efficient, making it easy to implement on hardware with minimal processing requirements, enabling rapid and accurate velocity adjustments.

These advantages also contribute to lower maintenance and equipment costs, particularly in high-precision and stability-critical systems. Therefore, implementing SMC for air curtain velocity control under dynamic pressure conditions not only enhances system performance but also optimizes cost efficiency.

This paper explores the enhancement of air condition management through the application of optimized air curtains, integrating the sliding mode control method to regulate airflow and maintain effective pollutant mass fraction. By adjusting the velocity of the air curtain in response to external disturbances, such as changing pressure and environmental parameters, the proposed system aims to maintain an optimal mass fraction of CO_2 and other pollutants. The findings demonstrate the potential of this innovative control strategy to significantly improve quality of the air condition, ensuring robust pollutant management and enhanced operational efficiency in enclosed spaces.

2- Navier-Stokes Equations/K-ω Shear Stress Transport (SST) Turbulence Model

In dynamic modeling, understanding fluid flow is crucial, as it forms the foundation for analyzing and predicting system behavior. The Navier-Stokes equations are used to describe the motion of fluids based on the principles of momentum conservation and continuity equation.

These equations are fundamental for predicting fluid behavior under various forces, particularly in turbulent flow conditions. The continuity equation presented in Eq. (1), ensures mass conservation within the flow field, where $\vec{v}$ denotes the fluid velocity vector.

$$\nabla \cdot \vec{v} = 0 \tag{1}$$

In this study, the two-dimensional incompressible Navier-Stokes momentum equations are employed. These equations account for the conservation of momentum in both the horizontal (x) and vertical (y) directions, incorporating effects of inertia, pressure gradients, and viscous diffusion as follows:

$$\rho\left(u\frac{\partial u}{\partial x}+v\frac{\partial u}{\partial y}\right) = -\frac{\partial p}{\partial x}+\frac{\partial}{\partial y}\left(\mu\frac{\partial u}{\partial y}\right)+\frac{\partial}{\partial y}\left(\mu_t\frac{\partial u}{\partial y}\right) \tag{2}$$

$$\rho\left(u\frac{\partial v}{\partial x}+v\frac{\partial v}{\partial y}\right) = -\frac{\partial p}{\partial y}+\frac{\partial}{\partial y}\left(\mu\frac{\partial v}{\partial y}\right)+\frac{\partial}{\partial y}\left(\mu_t\frac{\partial v}{\partial y}\right) \tag{3}$$

In these equations, u and v represent the velocity components in the horizontal (x) and vertical (y) directions, respectively; ρis the fluid density; P is the static pressure; μ is the dynamic (molecular) viscosity; and μ_t is the turbulent (eddy) viscosity, introduced to capture turbulence effects within the airflow. The convective terms on the left-hand side describe the inertial transport of momentum, while the right-hand side includes pressure gradients and the diffusion of momentum due to both molecular and turbulent viscosity in the vertical direction.

The k-ω SST turbulence model [10] is used for modeling the viscous sublayer of boundary layers due to its relative simplicity, strong numerical stability, and effectiveness in capturing

turbulence, especially in near-wall regions. It enables accurate prediction of mean velocity profiles without the need for empirical damping functions.

The modifications introduced by Wilcox [11] further enhance the model's capability to handle complex boundary conditions such as rough surfaces and surface mass injection. Although the model does not resolve detailed turbulence characteristics near the wall, this limitation is acceptable in regions where the eddy viscosity is significantly smaller than the molecular viscosity. As a result, the model remains effective in predicting mean flow behavior and wall shear stress with sufficient accuracy. It solves two transport equations: one for turbulent kinetic energy (k), which represents the energy contained in turbulence, and another for the specific dissipation rate (ω), which controls the rate of turbulence dissipation [11, 12].

3- Case Study

In order to obtain dynamic modeling based on numerical data, an enclosed space with length 58 (m) and height 4.8 (m), equipped with air curtain configuration is assumed as Figure 1. Note that the air curtain width (b) is selected as 0.2 (m).

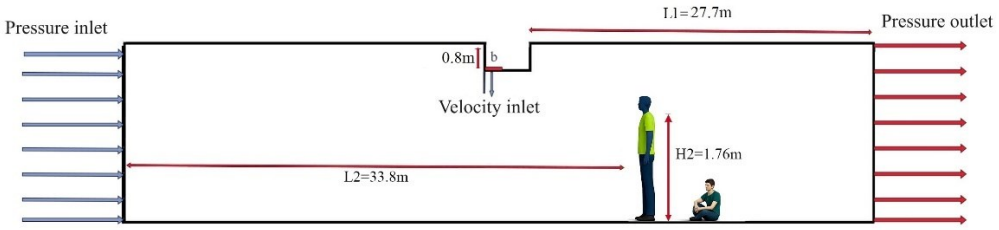

Fig.1 Configuration of the air curtain installed in the specified enclosed room and the position of the persons inside the room [13]

3.1- Boundary Conditions

The boundary conditions employed in this study include specified velocity inlets at the discharge nozzle, where a range of velocities is applied along with a turbulence intensity of 5%. All solid boundaries are modeled as zero-thickness, no-slip walls. On the left side of the computational domain, pressure boundary conditions of 0.5, 1.5, and 2.5 Pa are applied to represent dynamic pressure effects, while the static pressure reference is set to zero-gauge pressure. A pressure outlet condition is imposed on the right side of the domain, also with a turbulence intensity of 5% (see Figure 1). All simulations are carried out under isothermal conditions.

The working fluids considered in this study are air and carbon dioxide (CO_2), with CO_2 treated as the pollutant species. The mass diffusivity of CO_2 in air is taken as 0.16×10^{-4} (m^2/s). CO_2 gas is released from the left side of the air curtain at different pressures.

The primary function of the air curtain is to restrict the spread of CO_2 along the length of the room, maintaining adequate oxygen levels on the right side. If an individual is positioned either standing or sitting on the right side of the room (Figure 1), the air curtain adjusts to ensure the supply of oxygen instead of the pollutant gas, thereby creating a safer breathing environment.

To ensure the accuracy and robustness of the numerical framework, the validation was carried out using three independent and complementary datasets representing the dominant flow regimes relevant to air curtain operation.

First, free jet experimental data available in [14] were reproduced to evaluate the model capability in predicting jet development and velocity decay . The simulations were performed under steady Reynolds-averaged Navier–Stokes formulation using the same turbulence model, numerical schemes, and convergence criteria adopted in the main analysis. The predicted normalized velocity profiles along the jet centerline showed good agreement with the experimental measurements, with a mean deviation on the order of a few percent, confirming the reliability of the model in capturing free jet behavior (Figure 2 (a)).

Second, the numerical setup was assessed against an independent room-scale air curtain simulation reported in [1], focusing on airflow structure and pollutant transport under identical boundary conditions. The comparison of normalized velocity distributions demonstrated close consistency between the present predictions and the reference results, verifying the ability of the model to reproduce air curtain flow characteristics and separation performance in an enclosed environment (Figure 2 (b)).

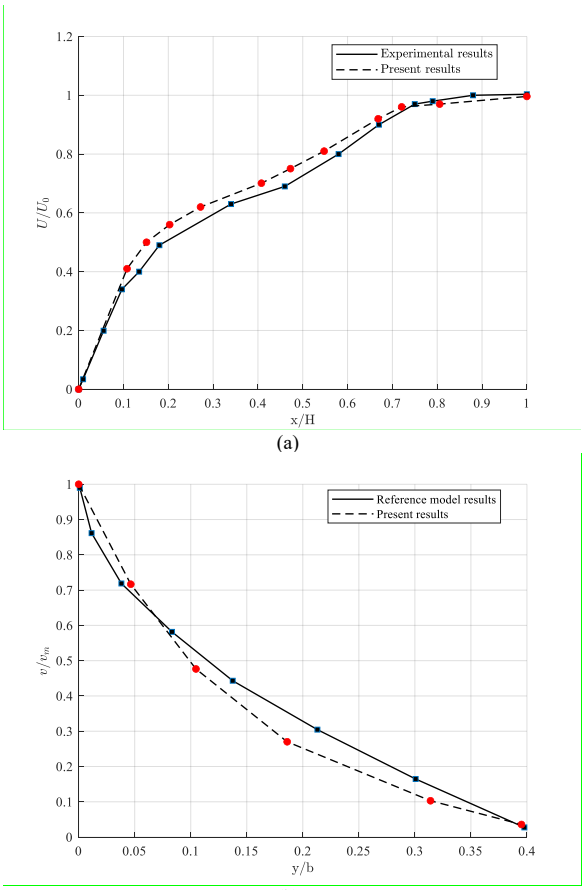

Fig.2 Comparison of jet velocity profile with (a) validation case in [14], (b) validation case in [1]

Third, experimental wall jet data in [15] were employed to validate near-wall flow behavior, which is critical for wall-mounted air curtain configurations. The numerical results closely matched the measured velocity profiles at multiple downstream locations, confirming that the selected turbulence model and near-wall resolution accurately capture wall jet dynamics. Further details are provided in [13].

Overall, the agreement obtained across free jet, wall jet, and room-scale air curtain datasets confirms the reliability of the adopted CFD methodology. These validations support the use of the steady-state numerical results as a dependable basis for extracting velocity–pollutant relationships and developing the

control-oriented model used in the subsequent closed-loop analysis.

3.2- Solver Setting and Computational Grid

The simulations are performed using ANSYS Fluent, where the two-dimensional Reynolds-averaged Navier-Stokes (RANS) equations are solved in conjunction with the k–ω SST turbulence model. Pressure-velocity coupling is handled using the SIMPLEC algorithm, consistent with methods commonly adopted in similar studies, and second-order accuracy is applied for pressure interpolation. All simulations are carried out under steady-state conditions. Convergence is considered achieved when the scaled residuals fall below 10^{-6} for the x and y momentum equations, 10^{-5} for turbulent kinetic energy (k) and specific dissipation rate (ω), and 10^{-4} for the continuity equation [13].

A structured mesh is employed in the simulations, generated by defining the geometry, boundary conditions, and flow regions. This mesh type is chosen for its ability to conform closely to the geometry, enabling better alignment with the flow features and improved accuracy in regions with complex gradients. Edge sizing techniques are applied to control mesh refinement, particularly along wall boundaries, ensuring consistency and structure throughout the domain.

Special attention is given to the near-wall regions, where the mesh is refined to adequately resolve the boundary layer, making it suitable for use with the k–ω SST turbulence model. A finer mesh is applied near the air curtain jet discharge to capture steep velocity gradients, while coarser meshing is used in regions with more uniform flow behavior. The wall jet mesh example is depicted in Figure 3.

A grid convergence study was performed to verify that the numerical predictions are not affected by spatial discretization. Several structured meshes with progressively increasing resolution were generated, spanning from a coarse grid to a highly refined configuration. For each mesh, the weighted mean CO_2 mass fraction was monitored as the primary assessment metric, since it directly reflects the pollutant containment performance of the air curtain (Table 1).

The results showed that mesh refinement led to diminishing changes in the predicted mass fraction beyond an intermediate resolution. Increasing the total number of cells above approximately 33150 cells produced negligible variation in the monitored quantity, while substantially increasing computational expense. Accordingly, this mesh resolution was adopted for all subsequent simulations. The selected grid (M2) provides adequate resolution in regions with strong gradients, including the air curtain jet discharge and the pollutant transport zone, while maintaining reasonable computational efficiency.

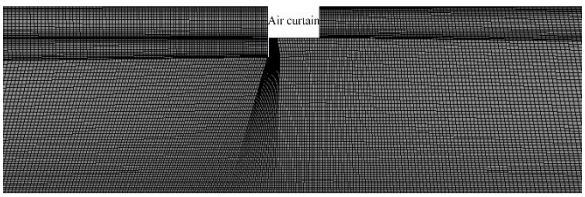

Fig.3 The wall jet mesh [13]

Table 1 Effect of mesh resolution on the CO_2 mass fraction

Mesh	Number of cells	CO_2 mass fraction
M1	20,640	1.0000
M2	33,150	0.0417
M3	40,530	0.0000
M4	57,070	0.0030

4- Contours of Pollutant Distribution under Various Pressure and Velocity Conditions

The mass fraction contours of CO_2 gas in the target room, are presented for the air curtain with jet width 0.2 (m) and pollutant inlet gas pressures of 0.5, 1.5, and 2.5 (Pa) [13] in Figures 4 and 5.

As the inlet pressure increases, the mass fraction of the pollutant gas also rises following the principles of the ideal gas laws, which leads to an increase in the air curtain jet velocity to mitigate the spread of the pollutant gas.

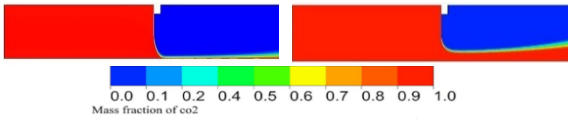

(a) (b)

Fig.4 Mass fraction contours of CO_2 at inlet pressures of (a) 0.5 (Pa), (b) 1.5 (Pa) with jet velocity of 2.5 (m/s) [13]

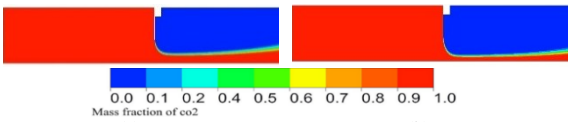

(a) (b)

Fig.5 Mass fraction contours of CO_2 at inlet pressure 2.5 (Pa), with jet velocities of (a) 3.5 (m/s), (b) 4.5 (m/s) [13]

5- Extraction of Mass Fraction Data

To control CO_2 mean mass fraction and adjust the air curtain jet velocity by the controller, it is necessary to send the mass fraction data to control system. According to the fact that mass fraction is a parameter spatially distributed in the room enclosure, it is not practical to implement all gathered information. So, a representative variable for describing this distribution is used. For this purpose, according to the contour plots in Figures 4 and 5, a proper section which is at 3.5 (m) horizontal distance from the air curtain, is selected. Accordingly, a set of mass fraction profiles as a function of room height are extracted from simulation data at this vertical section. The profiles are presented for three certain CO_2 inlet pressures (P) i.e. 0.5, 1.5, and 2.5 (Pa), at different curtain velocities (v) in Figure 6.

To realize this distribution, multiple sensors were strategically placed along the vertical wall of the enclosure at various heights in this section. These sensors were configured to measure the local mass fraction of CO_2 gas over time which will be used in the next section to evaluate the weighted mean mass fraction as a representative variable describing the CO_2 distribution.

Note that, the term ‘sensors’ refers to virtual sampling points (monitoring probes) defined within the CFD solution domain. These probes were placed at prescribed heights along the selected vertical section to record local CO_2 mass fraction values extracted from the converged simulation fields. For practical point of view, the actual sensors may be implemented in the given procedure to extract the necessary data.

By capturing the pollutant concentration at different vertical levels, this approach allows for a comprehensive assessment of pollutant dispersion dynamics within the enclosure.

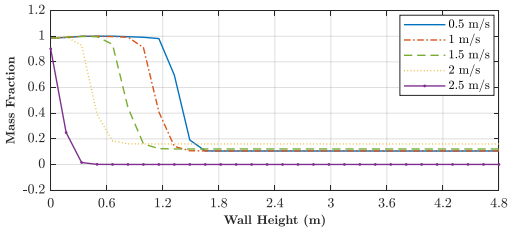

(a)

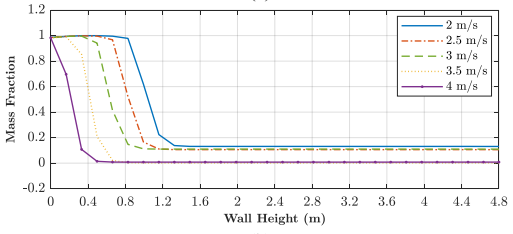

(b)

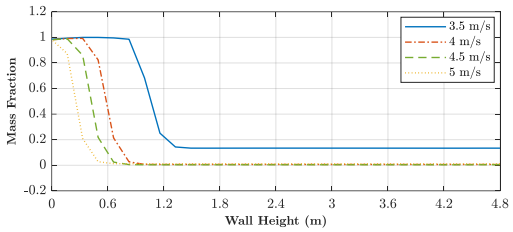

(c)

Fig.6 Mass fraction distribution at different room heights for a jet width of 0.2 m and inlet pressures of (a) 0.5 (Pa), (b) 1.5 (Pa), (c) 2.5 (Pa) at different air curtain velocities

6- Calculation of Weighted Mean Mass Fraction and Regression Analysis

The average CO_2 mass fraction ($\bar{m}$) based on the mass fraction values detected by the sensors (m_i) is calculated as a weighted mean to obtain a representative value of the overall pollutant present in the monitored zone as follows:

$$\bar{m} = \sum_{i=1}^{n} w_i m_i \; w_i = \frac{m_i}{\sum_{i=1}^{n} m_i} \tag{4}$$

where, w_i and n stand for weighing factor and number of sensors, respectively.

The next step involves interpolation based on mean mass fraction values. For this purpose, a nonlinear function $f_P(v)$ based on extracted mass fraction profiles is considered which maps jet velocity to steady state mass fraction at a given pressure P. So, a polynomial regression is employed to represent this relationship between air curtain velocity and the weighted mean CO_2 mass fraction at each pressure level. Several candidate polynomial orders were tested to capture the observed nonlinearity without introducing numerical artifacts. Lower-order polynomials were found to under-represent the curvature of the extracted data, while higher-order fits offered no meaningful improvement and increasing susceptibility to over-fitting and oscillatory behavior.

Table 2 summarizes the RMSE of polynomial interpolation for different polynomial orders under various inlet pressure conditions. Specifically for pressures of 1.5 (Pa) and 2.5 (Pa), the RMSE decreases noticeably up to intermediate polynomial orders, after which further increases in order do not lead to improvements. This trend indicates that higher-order polynomials do not yield substantial accuracy gains for these pressure levels and may introduce unnecessary numerical sensitivity and oscillations. Accordingly, a fourth-order polynomial was selected as a balanced choice to ensure adequate accuracy while avoiding overfitting across the studied pressure ranges.

Table 2 RMSE values of the regression polynomials with different orders

Order	Pressure (Pa) 0.5	1.5	2.5
1	0.0710	0.0537	0.0642
2	0.0696	0.0392	0.0427
3	0.0597	0.0294	0.0454
4	0.0836	0.0207	0.0424
5	0.0510	0.0218	0.0384
6	0.0501	0.0247	0.0444
7	0.0396	0.0286	0.0435

Based on this trade-off, the fourth-order model in Eq. (5) was adopted.

$$m_s = f_P(v) = a_0 + a_1 v + a_2 v^2 + a_3 v^3 + a_4 v^4 \tag{5}$$

where v denotes the airflow velocity. f_p is the interpolation mass fraction function for calculating mass (m_s), with a_0 to a_4 coefficients calculated for a specific pressure P which are reported in Table 3.

Table 3 Fourth-order regression function coefficients

Function coefficients	Pressure (Pa) 0.5	1.5	2.5
a_0	0.0031	0.0069	0.0073
a_1	-0.0182	-0.0650	-0.0829
a_2	-0.0003	0.1690	0.2914
a_3	-0.0022	-0.1485	-0.3665
a_4	0.3550	0.3380	0.4305

As the pressure changes, the system switches between different mass fraction functions, leading to changes in system dynamic. So, the dynamic model of the air curtain system can be expressed as the following differential equations:

$$\frac{dm_s}{dt} = \frac{\partial f_P(v)}{\partial v} \cdot \frac{dv}{dt} \tag{6}$$

7- Control System Structure Based on Sliding Mode Control (SMC)

In this section, the control structure and the design procedure of sliding mode control for controlling the mass fraction is presented.

The control system architecture is demonstrated in the schematic block diagram of Figure 7 including CO_2 dispersion and air curtain dynamics. The CO_2 dispersion dynamics consist of two blocks. The first block accounts for nonlinear relation between jet velocity and inlet pressure with mean mass fraction. The second block considers a first order transfer function $\frac{1}{1+\tau_m s}$ with time constant τ_m as dispersion time constant, which accounts for the time taken to the mass fraction reach its steady value after any change in jet velocity. The air curtain dynamics is also considered as a first order system with time constant τ_v, which accounts for the time taken to the jet velocity v(t) reach its steady value after any change in jet velocity command $v_s(t)$calculated by the control system.

Considering the controlled variable as CO_2 mass fraction, the feedback signal is selected as mean mass fraction m_o. Based on this, the controller adjusts air curtain speed by computing the jet velocity command $u(t) = v_s(t)$ using desired mass fraction (m_d) and measured mass fraction (m_o) data. It should be noted that, the CO_2 inlet pressure at this control structure is considered as disturbance input. For this purpose, the sliding mode control structure is considered.

In order to design the proposed sliding mode controller, first, a sliding surface is defined as Eq. (7) [9]:

$$s = \lambda_1 \dot{e}_s + \lambda_2 e_s \tag{7}$$
$$e_s = m_d - m_o$$

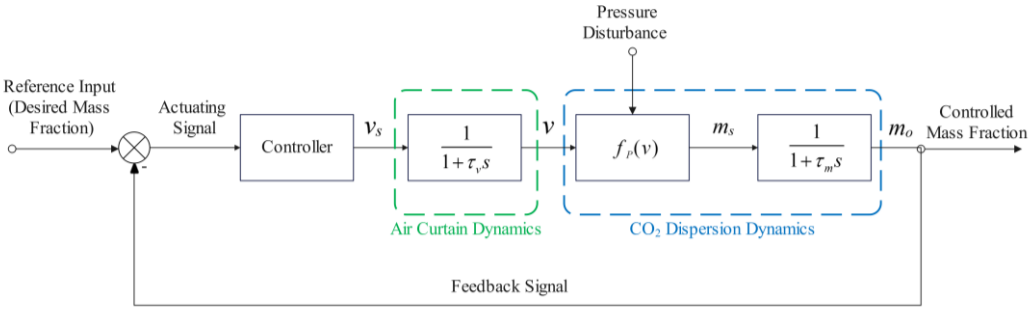

Fig.7 Closed-loop block diagram

where m_d is the desired mean mass fraction and m_o denotes the controlled mean mass fraction with the e_s being the output error. $\lambda_1$and λ_2 represent sliding surface design parameters which are selected as positive constants to shape the error dynamics and ensure a fast yet non-oscillatory convergence. In the simulations reported in this study, the controller parameters were set to λ_1=1 and λ_2= 10. These values were chosen to balance settling time and robustness against pressure-induced disturbances while avoiding excessive control activity.

In the next step, the sliding surface dynamics may be written as Eq. (8).

$$\begin{aligned}\dot{s} &= \lambda_1 \ddot{e}_s + \lambda_2 \dot{e}_s \\ &= \lambda_1(\ddot{m}_d - \ddot{m}_o) + \lambda_2(\dot{m}_d - \dot{m}_o) \\ &= \lambda_1 \ddot{m}_d - \lambda_1\left(\frac{1}{\tau_m}(\dot{m}_s - \dot{m}_o)\right) + \lambda_2 \dot{m}_d - \lambda_2 \dot{m}_o \\ &= \underbrace{\lambda_1 \ddot{m}_d + \lambda_2 \dot{m}_d}_{\varphi} - \frac{\lambda_1}{\tau_m}\frac{\partial f_P}{\partial v}\frac{1}{\tau_v}(u - v) \\ &+ \frac{1}{\tau_m}\left(\frac{\lambda_1}{\tau_m} - \lambda_2\right)(m_s - m_o) \\ &= w + \varphi\end{aligned} \tag{8}$$

Where w is a virtual input and φ stands for disturbances and uncertain terms compensated by sliding mode controller. So, the control law may be obtained as follows:

$$u = v + \frac{\tau_v}{\lambda_1}\left(\frac{\partial f_P}{\partial v}\right)^{-1}\left(\left(\frac{\lambda_1}{\tau_m} - \lambda_2\right)(m_s - m_o) - \tau_m w\right) \tag{9}$$

By assuming w= -η sgn(s), it may be shown that by using a proper Lyapunov function [9], an appropriate scalar function η may be selected so that the proposed control law makes the sliding surface approach zero in finite time and guarantees the stability of the sliding motion and hence the output error e_s.

This also ensures that mass fraction reaches to the desired value asymptotically. Note that to reduce the chattering, a common phenomenon occurred in sliding mode-controlled systems due to switching behavior of sign function, the saturation function is implemented instead.

8- Results and Discussions

In this section, the performance of the proposed sliding mode control strategy is evaluated through numerical simulations under varying pressure conditions.

The primary objective is to assess the effectiveness of the optimized air curtain in maintaining pollutant containment while adapting to different pressure conditions. The air curtain velocities v_s and controlled pollutant mass fractions (m_o) at three different pressures 0.5 (Pa), 1.5 (Pa), and 2.5 (Pa) are shown in Figure 8.

As expected, higher pressure levels lead to an increase in required air curtain velocity to effectively control the pollutant gas, reflecting the need for stronger airflow to prevent pollutant penetration.

The sliding mode controller (SMC) effectively regulates the velocity to maintain stability, ensuring that even under different pressure values, the system controls mass fraction effectively, so that the mass fraction in all three pressure scenarios, reaches to desired value (0.15) in almost 1000 sec, and the SMC quickly stabilizes the system, ensuring pollutant containment within acceptable limits.

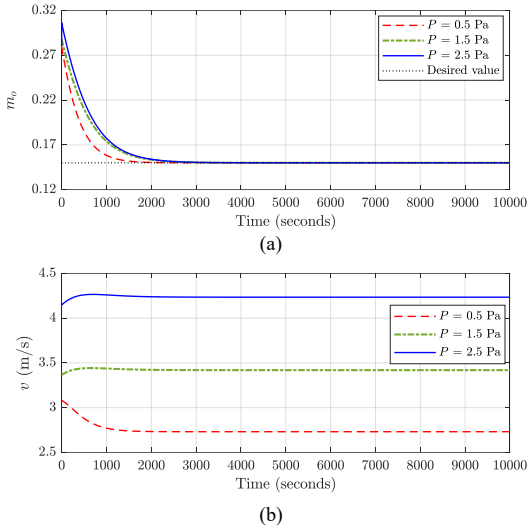

Fig.8 (a) mass fraction, m_o , (b) jet velocity, v (m/s),

The results indicate that despite increasing pressure, the air curtain maintains a controlled pollutant mass fraction, demonstrating the robustness of the proposed control strategy.

The results also confirm the low delay time, ensuring fast convergence to the desired mass fraction value. Also, no overshoot is observed in all different pressure scenarios. The tracking error is also negligible, which guarantees the accurate mass fraction control. The calculated jet velocities by the control method are reasonable and in the functional range, which may be provided in order to create desired pollutant mass fraction values.

Additionally, the effect of pressure variations as external disturbances on both the jet velocity and mass fraction is investigated to demonstrate the robustness of the designed controller. The results are presented in Figure 9. It is assumed that the pressure experiences changes from 1.5 to 2.5 (Pa) and back to 2.5 (Pa) (Figure 9 (a)).

The Figure 9 (b) shows that the jet velocity v is effectively regulated to compensate rapid pressure changes regarded as disturbances, in order to control mass fraction. It is obvious that by increasing pressure, higher values of jet velocity should be provided.

The results in Figure 9 (c) indicates that the control system effectively controls mass fraction in the presence of pressure sudden variation, so that the closed loop system outputs reach the desired value (0.15) in finite time smoothly.

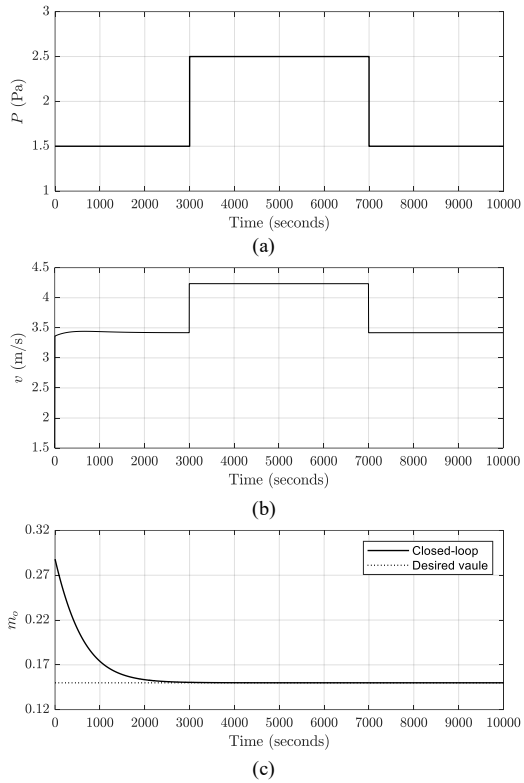

Fig.9 (a) The pressure variation P (Pa), (b) jet velocity v (m/s), (c) mass fraction, m_o

Overall, the simulation results confirm that despite dynamic pressure variations, the control strategy ensures stability and effective pollutant containment, demonstrating its robustness against environmental fluctuations. These results support the effectiveness of the sliding mode control in dynamically adjusting air curtain velocity to maintain the quality of the air condition in enclosed spaces under varying pressure conditions.

9- Conclusion

This study presents an automated air curtain system integrated with a sliding mode control (SMC) strategy to enhance air condition management in enclosed spaces. Through detailed numerical simulations, the effectiveness of the proposed control system was evaluated under different pressure conditions acting as external disturbances. The results demonstrated that the SMC effectively regulates the air curtain velocity to maintain a stable pollutant mass fraction, ensuring robust containment of CO_2 gas despite varying environmental conditions. The findings highlight the advantages of SMC in handling disturbances, providing rapid adjustments to pressure fluctuations while maintaining system stability. Ultimately, the proposed approach exhibited appropriate performance in pollutant containment and response time, making it a viable solution for dynamic air condition control applications.

Ethical Statement

The content of this manuscript is original, based on the authors' research, and has not been published or submitted elsewhere, either in Iranian or international journals.

Conflict of interest

The authors declared that they have no conflicts of interest to this work.

Funding

No external funding was received for this study.

References

[1] Khayrullina, A., Blocken, B., de Almeida, M.O.M., van Hooff, T., van Heijst, G.: Impact of a wall downstream of an air curtain nozzle on air curtain separation efficiency. Building and Environment. 197, 107873 (2021). doi: 10.1016/j.buildenv.2021.107873.

[2] Ji, J., Lu, W., Li, F., Cui, X.: Experimental and numerical simulation on smoke control effect and key parameters of Push-pull air curtain in tunnel fire. Tunnelling and Underground Space Technology. 121, 104323 (2022). doi: 10.1016/j.tust.2021.104323.

[3] Safarzadeh, M., Heidarinejad, G., Pasdarshahri, H.: The effect of vertical and horizontal air curtain on smoke and heat control in the multi-storey building. Journal of Building Engineering. 40, 102347 (2021). doi: 10.1016/j.jobe.2021.102347.

[4] Safarzadeh, M., Heidarinejad, G., Pasdarshahri, H.: Air curtain to control smoke and fire spread in a ventilated multi-floor building. International Journal of Thermal Sciences.159,106612(2021). doi: 10.1016/j.ijthermalsci.2020.106612 .

[5] Yu, L., Chen, Y., Chen, S., Zhang, Y., Zhang, H., Liu, C.: Numerical analysis of the performance of a PID-controlled air curtain for fire-induced smoke confinement in a tunnel configuration. Fire Safety Journal. 141, 103930 (2023). doi: 10.1016/j.firesaf.2023.103930.

[6] ZHANG, L., YAN, Z.-z., LI, Z.-h., WANG, X.-m., HAN, X.-f., JIANG, J.-c.: Study on the effect of the jet speed of air curtain on smoke control in tunnel. Procedia engineering.211,1026–33(2018). doi: 10.1016/j.proeng.2017.12.106.

[7] Viegas, J.: Saltwater experiments with air curtains for smoke control in the event of fire. Journal of Building Engineering.8,243–8(2016). doi: 10.1016/j.jobe.2016.08.008.

[8] Zhang, T., Han, R.: Numerical study on the influence of subway platform air curtains on smoke diffusion. Case Studies in Thermal Engineering. 50, 103439 (2023). doi: 10.1016/j.csite.2023.103439.

[9] Shtessel, Y., Edwards, C., Fridman, L., Levant, A.: Sliding mode control and observation. Springer (2014). doi: 10.1007/978-0-8176-4893-0.

[10] Wilcox, D.C.: Turbulence modeling for CFD. 3rd ed. DCW industries La Canada, CA (2006). doi:

[11] Wilcox, D.C.: Reassessment of the scale-determining equation for advanced turbulence models. AIAA journal. 26(11), 1299–310 (1998). doi: 10.2514/3.10041.

[12] Menter, F.R.: Two-equation eddy-viscosity turbulence models for engineering applications. AIAA journal. 32(8), 1598–605 (1994). doi: 10.2514/3.12149.

[13] Babazadeh Asbagh, G.: Numerical investigation of the effect of different parameters in preventing the emission of polluting gasses in a room using air curtains. Msc Dissertation, University of Tabriz (2024).

[14] Maurel, S., Solliec, C.: A turbulent plane jet impinging nearby and far from a flat plate. Experiments in Fluids. 31(6),687–96(2001).doi: 10.1007/s003480100327.

[15] Eriksson, J., Karlsson, R., Persson, J.: An experimental study of a two-dimensional plane turbulent wall jet. Experiments in fluids. 25(1), 50–60 (1998). doi: 10.1007/s003480050207.